ELSEVIER

Organic Electronics 2 (2001) 53–62

Organic Electronics

www.elsevier.nl/locate/orgel

Molecularly doped polymer light emitting diodes utilizing phosphorescent Pt(II) and Ir(III) dopants

Sergey Lamansky, Raymond C. Kwong [1], Matthew Nugent[1], Peter I. Djurovich, Mark E. Thompson *

Department of Chemistry, University of Southern California, Los Angeles, CA 90089, USA

Received 11 October 2000; accepted 16 January 2001

Abstract

The use of molecular phosphorescent dyes in polymer-based organic light emitting diodes (OLED) of different architectures was investigated by incorporating several phosphorescent dopants into poly(*N*-vinylcarbazole) (PVK)-based single layer and single heterostructure light emitting diodes (LEDs). In particular, *cis*-bis[2-(2-thienyl)pyridine-N,C^3] platinum(II) ($Pt(thpy)_2$) and platinum(II) 2,8,12,17-tetraethyl-3,7,13,18-tetramethyl porphyrin (PtOX), and an Ir(III) compound, *fac*-tris[2-(4′,5′-difluorophenyl)pyridine-C'^2,N] iridium(III) (FIrppy) were used. The maximum external quantum efficiency of phosphorescent devices exceeds 0.6% for the two Pt dopants and reaches ≈1.8% for FIrppy. An overall increase in LED efficiency compared to similar devices based on fluorescence is attributed to the fact that phosphorescent dopants allow both singlet and triplet excitons to be involved in emission. In addition to finding an energetically suitable dopant, such parameters as dopant concentration and organic layer thickness influence the performance of the LEDs. Introduction of an electron injecting layer of tris(8-hydroxyquinoline) aluminum(III) causes an increase of quantum efficiency of up to 1.8–2.8%. The second order quenching process present in these OLEDs, which is prevalent at high current densities, is most likely not due to T–T annihilation of excitons trapped at dopant sites in these OLEDs. T–T annihilation in the PVK matrix or trapped charge-triplet annihilation are more likely explanations for the decrease.

Keywords: OLED; Light emitting diode; Phosphorescence; High efficiency; Electroluminescence; Polymer

1. Introduction

The performance of an organic light emitting diode (OLED) is controlled by several parameters, many of which can be affected by simple changes at molecular level. The photoluminescence quantum yield of the emitting molecules (Φ_{pl}) and fraction of excitons that can induce *radiative* electron–hole recombination (χ) are two such parameters [1]. The product of these two parameters ($\phi_{pl} \bullet \chi$) sets an upper limit on device efficiency. χ can be maximized by choosing phosphorescent emitters, since they efficiently trap both singlet and triplet excitons (i.e. $\chi = 1$) [2–5]. In contrast, the use of fluorescent emitters severely limits light emitting diode (LED) efficiency, since $\chi \approx 0.25$ (only 1/4 of the excitons formed in the EL process

* Corresponding author.
E-mail address: met@usc.edu (M.E. Thompson).
[1] Present address: Universal Display Corporation, Ewing, NJ 08618, USA.

1566-1199/01/$ - see front matter
PII: S1566-1199(01)00007-6

are singlets) [6]. Recent reports suggest that the fraction of singlet excitons may be higher in OLEDs built with conjugated polymers [7,8], however, the reported χ is still <0.5, providing a restriction on the possible efficiency of the device. The phosphorescent doping concept has been used to prepare molecular OLEDs doped with highly efficient phosphorescent Ir complex, iridium(III) *fac*-tris(2-phenylpyridinato-N,$C^{2\prime}$) [Irppy], which gave an external quantum efficiency of 15.5% [4]. Considering that the maximum possible external efficiency for a device of this structure is 20% [9], the 15.5% value comes very close to the maximum achievable efficiency. Similar efficiencies have never been accomplished with fluorescence-based devices, even when dyes were chosen with $\phi_{pl} = 1.0$.

In spite of the advances in phosphorescent doping of molecular, vacuum-deposited OLEDs, only a limited number of polymer-based devices which incorporate phosphorescent dopants have been reported [10–13]. Our goal in this paper is to investigate this class of polymer based devices further. Molecularly doped polymer (mdpLEDs) devices are a convenient device architecture to study phosphorescent polymer LEDs due to the relative ease of preparation and availability of carrier transporting polymeric and molecular materials [14,16]. In mdpLEDs either inert or carrier transporting polymer are doped with molecular materials, which are chosen to show efficient emission and/or carrier transport. One of the most commonly used polymers in mdpLEDs is poly(*N*-vinylcarbazole) (PVK), due to its excellent film-forming properties, high glass transition temperature, wide energy gap (emission is observed in the blue spectral region) and good hole mobility of $\approx 10^{-5}$ $cm^2\,V^{-1}\,s^{-1}$, at the electric fields typical for OLEDs (10^6 $V\,cm^{-1}$) [15]. Electron transporting molecules and emitting dopants are either dispersed in PVK matrix to form a single-layer device or vacuum-deposited on top of the PVK film to form an organic/polymer heterostructure. To date the best examples of both single-layer and heterostructure fluorescent doped PVK-based LEDs show peak external quantum efficiency of about 1.1% [16,17]. Huang et al., developed one of the best fluorescence-based single-layer mdpLEDs (peak quantum efficiency 1.2%) by doping electron transporting 2-(4-biphenyl)-5-(4-tert-butylphenyl)-1,3,4-oxadiazole (PBD) and poly(2,5-dibutyloxyphenylene) into PVK [18]. Examples of PVK-based mdpLEDs with phosphorescent dopants, i.e. lanthanide [19,21], Os [20], Au and Cu [22] complexes, have been reported, however, they give electroluminescence efficiencies of 0.1% or less, which are lower than would be expected from their phosphorescence quantum yields. Very recently efficient multilayer devices, with Irppy doped into a hole transporting polymer layer, have been reported [13].

Here we report a preparation of efficient PVK-based single-layer devices incorporating electron transporting PBD and phosphorescent complexes of platinum(II) or iridium(III). Two of the studied compounds, *cis*-bis[2-(2-thienyl)pyridine-N,C^3] platinum(II) ($Pt(thpy)_2$) and *fac*-tris[2-(4′,5′-difluorophenyl)pyridine-N,C'^2] iridium(III) (FIrppy), belong to the class of homoleptic *ortho*-metalated complexes. The third in the series of studied complexes, platinum(II) 2,8,12,17-tetraethyl-3,7,13,18-tetramethyl porphyrin (PtOX), represents a class of metal porphyrins. Both types of metal complexes often show strong emission originating from their triplet metal-to-ligand charge transfer (^{3}MLCT) and intraligand (^{3}LL) excited states in solution and/or in the solid state [23,24]. The triplet excited state energy is different for these dopants decreasing in the series FIrppy > $Pt(thpy)_2$ > PtOX (phosphorescence maxima at ≈510, 580 and 650 nm, respectively). Both single-layer OLED architecture (ITO/PVK–PBD–dye/Mg–Ag/Ag) and molecularly doped polymer/organic heterostructure architecture (ITO/PVK–PBD–dye/Alq_3/Mg–Ag/Ag) are used in this study, and the factors that govern electroluminescence efficiency in such LEDs are investigated.

2. Experimental

2.1. Synthesis

All solvents, PVK (**4**, Fig. 1), PBD (**5**, Fig. 1) were purchased from Sigma-Aldrich. All except for the later were used as received. PBD was re-

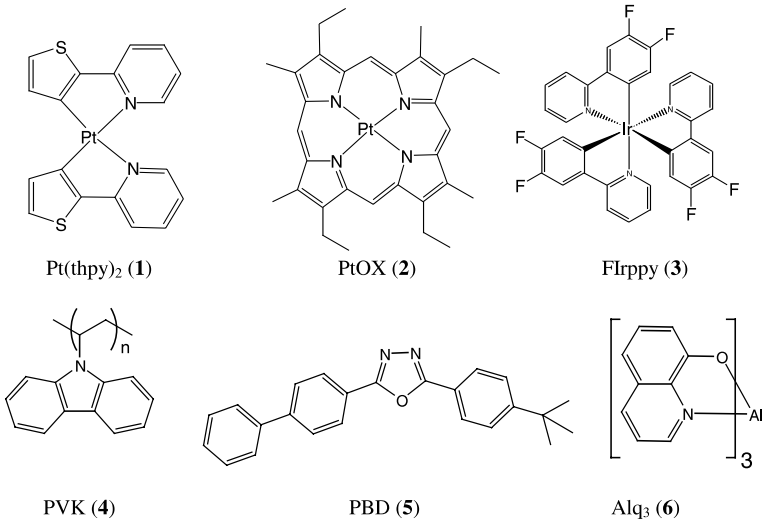

Fig. 1. Chemical structures of used compounds.

sublimed prior to use. $Pt(thpy)_2$ (**1**, Fig. 1) was synthesized by transmetalation reaction between *trans*-di(diethylsulfide)dichloride platinum(II) and 3′-(2-(2′-thienyl)pyridine) lithium reported by von Zelewsky and Chassot [25]. PtOX, platinum(II) 2,8,12,17-tetraethyl-3,7,13,18-tetramethyl porphyrin was prepared according to Kwong et al. [23]. 2-(4′,5′-difluorophenyl)pyridine was prepared by Negishi et al. coupling of the corresponding aryl bromides [26]. ^{1}H NMR spectra were recorded on Bruker AMX 500 MHz spectrometer. Mass spectra were monitored on Hewlett Packard spectrometer with series 5973 MSD.

FIrppy (**1**, Fig. 1) was synthesized according to Watts and coworkers [27]. ^{1}H NMR (500 MHz, $CDCl_3$), ppm: 8.35 (m,3H), 7.68 (m,3H), 7.52 (m,3H), 6.93 (m,3H), 6.67 (m,3H), 6.37 (m,3H). MS, m/z: 763 (M^+, 100%), 762 (83%), 761 (58%), 760 (43%), 571 (21%), 382 (17%). Elem. Anal.: calc C, 51.97; H, 2.38, N, 5.51; found C, 51.93; H, 2.39; N, 5.57.

2.2. Optical measurements

Absorption spectra were recorded on AVIV model 14DS-UV–VIS–IR spectrophotometer (re-engineered Cary 14) and corrected for background due to solvent absorption. Emission spectra were recorded on PTI QuantaMaster™ Model C-60SE spectrofluorometer with 928 PMT detector and corrected for detector sensitivity inhomogeneity. Emission quantum yields were determined using *fac*-$Ir(ppy)_3$ as a reference [28].

2.3. LED and thin film preparation and testing

Polymer blend LEDs and thin films for AFM, ellipsometry, and photoluminescence study were spun coat from chloroform solution on patterned pre-cleaned and oxygen plasma treated indium tin oxide (ITO) coated glass substrates and covered with vacuum-deposited Mg:Ag (10:1 weight ratio) cathode (500 Å). Typically, 7.5 ml of a chloroform solution contained 100 mg of PVK, 40 mg of PBD and variable amount (0.5–2.5 mg) of a dye ($Pt(thpy)_2$, PtOX or FIrppy). Chosen spin-coating conditions (3000 RPM, 40 s, Specialty Coating Systems, Inc.) led to 1300 ± 20 Å-thick PVK:PBD:dye films as determined by ellipsometry (Rudolph automatic ellipsometer equipped with a He:Ne laser). Prior to spinning, the solutions were filtered through a 0.2 μm filter. Tris(8-hydroxyquinoline) aluminum(III) (Sigma-Aldrich, Inc.) (Alq_3) was sublimed prior to use. All measurements on the devices were carried out in air at room temperature. Device current–voltage and light intensity characteristics were measured using the LabVIEW™ program by National Instruments

Table 1
Absorption, excitation and photoluminescence parameters of $Pt(thpy)_2$ **1**, PtOX **2** [23] and FIrppy **3** in their toluene solutions (tol) and polystyrene solid matrix (PS)

Compound	Absorption λ_{max}, nm (log ε)	Emission λ_{max}, nm	Emission quantum yield ϕ_{pl}	Emission lifetime τ, μs	Excitation λ_{max}, nm
1 [40][a]	295 (4.9)	578 (tol)	0.18 ± 0.05 (tol)	2.0 ± 0.2 (tol)	390 (tol)
	405 (4.2)	580 (PS)		6.4 ± 0.4(PS)	390 (PS)
2	380 (5.3)	648 (tol)	0.44 ± 0.08 (tol)	76 ± 3 (tol)	390 (tol)
	501 (4.1)	648 (PS)		92 ± 2 (PS)	390 (PS)
	535 (4.6)				
3	290 (4.5)	505 (tol)	0.22 ± 0.05 (tol)	1.5 ± 0.1 (tol)	390 (tol)
	380 (3.8)	500 (PS)		4.5 ± 0.8 (PS)	390 (PS)

[a] The photophysics of $Pt(thpy)_2$ has been reported for acetonitrile solutions: λ_{max} (abs.) = 303 (ε = 26100) and 418 (ε = 10500) nm, λ_{max} (emission) = 578 nm with the lifetime of 2.2 μs.

with a Keithley 2400 Source Meter/2000 multimeter coupled to a Newport 1835-C optical meter.

Electroluminescence spectra were recorded at room temperature on a PTI QuantaMaster™ model C-60SE spectrofluorometer. Atomic force microscopy images were taken on a Digital Instrument NanoScope III model microscope using intermittent contact mode of acquisition.

3. Results and discussion

Although the use of phosphorescent dopants proved to be advantageous in molecular OLEDs, there are only a few reports of improved efficiency of electrophosphorescent polymer-based devices compared to the ones based solely on fluorescence [8,29]. Considering the amount of interest that has been shown in developing highly efficient polymer LEDs, it would be beneficial to determine if phosphorescent dopants can improve the performance of these devices. The mdpLEDs studied here include a single polymer layer of the hole transporting PVK, (**4**) with both an electron transporting organic molecule PBD (**5**) and a phosphorescent iridium(III) or platinum(II) complex (**1**–**3**) dispersed in it (Fig. 1). An important requirement for mdpLED materials is that they all show good solubility in organic solvents used for spin-coating the polymer films and good compatibility with the polymer. These requirements, in combination with long-term chemical stability and electronic properties of the component materials, control the performance and reliability of the devices. Although the hole mobility of PVK in its blends with molecular electron transporting (ET) materials has been shown to decrease with an increasing content of ET molecules [15], they can still exhibit an appreciable hole mobility ($\approx 10^{-6}$–10^{-5} $cm^2\,V^{-1}\,s^{-1}$ at 10^6 $V\,cm^{-1}$) [15]. In turn, electron mobility in the PBD-polycarbonate polymer films reaches 10^{-6}–10^{-7} $cm^2\,V^{-1}\,s^{-1}$ at an applied field of 10^6 $V\,cm^{-1}$, common for OLEDs [30].

3.1. Optical properties of dyes

The absorption and emission characteristics of $Pt(thpy)_2$, PtOX and FIrppy [2] are summarized in Table 1. In addition to intense π–π^* absorption bands at $\approx$300 nm, both **1** ($Pt(thpy)_2$) and **3** (FIrppy) display low energy absorption bands at 380–420 nm attributed to MLCT transitions. PtOX shows π–π^* and n–π^* absorptions typical for porphyrins at 380 nm (Soret band) and 501 and 535 nm (Q-bands), respectively. When excited at their absorption maxima, $Pt(thpy)_2$, PtOX and FIrppy exhibit efficient room temperature phosphorescence at 578, 648 and 502 nm, respectively, in either toluene solutions or as doped polystyrene thin films. Although excitation of either π–π^* or

[2] Despite very promising performance of underivatized Irppy in vacuum-deposited molecular LEDs (e.g. see [3]), it does not exhibit solubility in chloroform sufficient for its use for polymer blend LEDs. In turn, hexafluorinated Irppy, FIrppy, exhibits similarly good emission characteristics in combination with significantly increased solubility.

MLCT absorption bands can be used to promote phosphorescence in these complexes, corresponding excitation spectra show maxima centered close to the MLCT bands. In polystyrene thin films, emission lifetimes of **1**, **2** and **3** increase significantly relative to solution lifetimes, reaching 6.4, 92 and 4.5 μs, respectively. Although photoluminescence quantum yields in polystyrene:dye films were not measured directly, an increase in the luminescent lifetimes indicates the likelihood of higher emission efficiencies in the solid matrix due to the stabilization of the phosphorescent molecules in a rigid environment and a reduction of intermolecular interactions that lead to non-radiative decay processes.

The broad emission from a PVK thin film centered at 415–425 nm is attributed to delayed excimer fluorescence [31]. At 77 K, PVK films show long-lived phosphorescence at ≈500 nm [31]. It has been demonstrated that this phosphorescence is one of the components of room temperature emission of PVK thin films [32]. This emission energy is higher than phosphorescence energies observed for **1**, **2** and **3**. Therefore, S_1 and T_1 states in PVK are expected to be higher in energy than phosphorescent dye T_1 states, which is important to ensure efficient energy transfer from PVK to **1**, **2** and **3**. Photoluminescence studies on PVK-**1** thin films with variable dopant concentrations reveal efficient energy transfer to **1** over a range of concentrations, ≈4–9% by weight, with an optimal doping concentration of 6% **1** (Fig. 2). Upon excitation of PVK-**1** film with 4–9% concentration of **1** at the PVK absorption maximum (250 nm), predominant dye emission is observed, with only a minor contribution from PVK. Thin films with $Pt(thpy)_2$ amounts higher than 6% exhibit a decrease in the dopant phosphorescence intensity due to enhanced self-quenching.

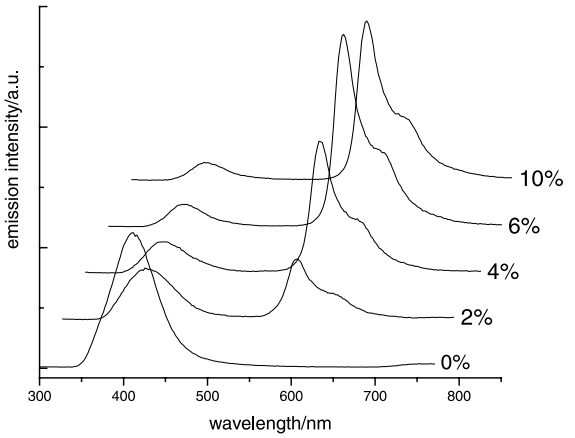

Fig. 2. Photoluminescence of $Pt(thpy)_2$ **(1)** embedded in the PVK matrix with variable complex content. Excitation wavelength corresponds to one of the absorption peaks of PVK (250 nm).

3.2. Single-layer light emitting devices

Single-layer mdpLEDs are one of the architecturally simplest light emitting structures, consisting of a single polymer PVK–PBD-phosphor layer, sandwiched between an ITO anode and a Mg–Ag cathode. A silver layer is added to the Mg–Ag cathode to retard aerobic degradation of the cathode, to give a general device structure of ITO/doped polymer layer/Mg–Ag/Ag.

The first complex we examined in mdpLEDs was $Pt(thpy)_2$ (**1**). The absorption spectrum of this phosphor has excellent spectral overlap with the PVK emission spectrum ensuring efficient energy transfer of PVK excitons to **1** (Fig. 2) [33]. This complex cannot be used for vacuum-deposited molecular based LEDs, since it partially decomposes upon sublimation, even at high vacuum. [3] Previous optimization of PVK–PBD structures with fluorescent dopants revealed that the best devices were obtained from a chloroform solution containing ≈13 mg/ml of PVK (**4**) and 5 mg/ml of PBD (**5**) [16]. Fluorescence-based LEDs are typically prepared with low doping levels of the fluorescent dye (≈0.5–1.5% by weight). The Förster energy transfer process is an efficient, long-range process, often being facile at host exciton-to-dye distances of 40 Å or more [33]. The energy transfer process typically observed for a triplet host exciton

[3] Although co-deposited in vacuum film of **1** with di(carbazole)biphenyl (CBP) exhibits emission at 578 nm corresponding to the phosphorescence of **1**, elemental analysis of the residue after deposition reveals following Pt/C composition: Pt 84.4, C 11.0, whereas in the pure starting **1** used for deposition Pt/C content shows Pt 43.9 and C 53.6 (cacl. Pt 43.60, C 53.69) indicating partial decomposition of **1**.

with low luminance efficiency, as expected for PVK excitons, is short-range Dexter (electron exchange) energy transfer process. The short-range nature of this transfer process, along with expected saturation effects, requires the use of substantially higher phosphorescent dopant concentrations (≈5–7 wt.%) [34].

ITO/PVK–PBD-**1**/Mg–Ag/Ag mdpLEDs exhibit electroluminescence with a peak corresponding to the dopant emission maximum at 580 nm (Fig. 4). PVK–PBD-**1** mdpLEDs were optimized for both phosphor concentration and thickness of the device. In particular, the devices were prepared with 1, 2, 2.7, 3.3 and 4 wt.% of **1** (determined as ratios of **1** to the total organic material in the film, PVK + PBD + dopant). The film thicknesses for all of these devices were held constant at 1300 Å. Fig. 3 shows current density–voltage and light output-voltage characteristics for all PVK–PBD-**1** mdpLEDs. Under the chosen deposition conditions, the devices show turn on voltages ($V_{\text{turn on}}$, Table 2) of ≈10–11 V for all $Pt(thpy)_2$ loadings. We define the turn on voltages as the voltage at which the light level measured at the optical power meter rises above 10^{-9} W (≈0.1 Cd m^{-2} for this dopant).

Despite high turn-on voltage, the ITO/PVK–PBD-**1** (1300 Å)/Mg–Ag/Ag devices reach quantum efficiencies comparable to those of PVK:PBD

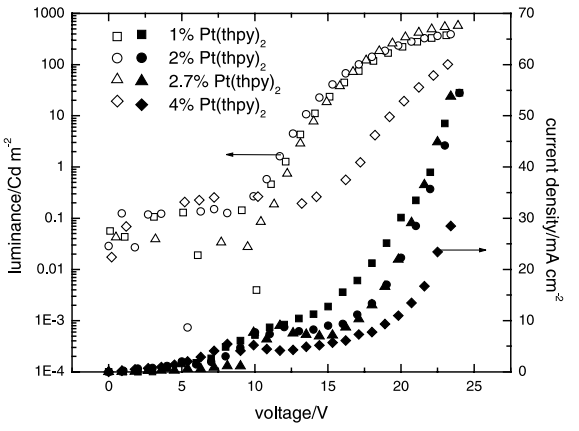

Fig. 3. Luminance (□, ○, △, ◇) and current density (■, ●, ▲, ◆) characteristics of 1%, 2%, 2.7% and 4%-doped ITO/PVK–PBD–$Pt(thpy)_2$/Mg–Ag/Ag devices as functions of applied voltage.

Table 2
Characteristics of ITO/PVK–PBD–dopant/Mg–Ag/Ag mdpLEDs. Listed quantum efficiencies are external quantum efficiencies (photons/injected electrons)

Dopant	Dopant concentration, %	Thickness, Å	$V_{\text{turn on}}$, V	Peak q.e., %
1	1	1300	10	0.33
1	2	1300	10	0.42
1	2.7	1300	11	0.53
1	3.3	1300	10	0.61
1	4	1300	11	0.26
1	3.3	1000	8	0.71
1	3.3	1100	8.5	0.67
1	3.3	1300	10	0.61
1	3.3	1700	11	0.58
2	0.6	1300	12	0.21
2	1.3	1300	10	0.52
2	2.1	1300	9	0.62
2	3.3	1300	9	0.48
3	0.7	1300	11	0.41
3	1.4	1300	9	0.98
3	2.2	1300	9	1.71
3	3.5	1300	8	1.78

devices with the best fluorescent dyes [16]. Current density values corresponding to peak quantum efficiencies are in the range typical for molecular OLEDs (5–20 mA cm^{-2}). Maximum quantum efficiencies of ITO/PVK–PBD-**1** (1300 Å)/Mg–Ag/Ag devices increased from 0.33% at 0.61% as the doping level was raised from 0.61% to 3.3% (Table 2). When the doping level was increased to 4% the quantum efficiency decreased to 0.26%. The drop in efficiency can be attributed to increasing self-quenching at higher phosphor loadings. High driving voltages contribute to the low power efficiencies for these devices (less than 0.5 lm/W), as has been observed for other reported mdpLEDs [16]. Brightness of the devices at the peak efficiency range from 300 to 500 Cd m^{-2} whereas maximum brightness of more than 1000 Cd m^{-2} is typically achieved at higher voltages.

A study of the variation on LED performance with film thickness was performed on PVK–PBD-**1** (3.3%) devices with organic layers that ranged from 1000 to 1700 Å. In this thickness range the PVK–PBD-**1** films exhibit highly uniform morphology with an average roughness of ≈10–40 Å based on AFM measurements. In this range of polymer layer thickness, the light emitting struc-

tures exhibited only slight variation in luminous efficiencies. Thus, the quantum efficiency of ITO/PVK–PBD-**1** (3.3%)/Mg–Ag/Ag mdpLEDs decreases from 0.71% at 1000 Å-thick PVK-based layer to only 0.58% at 1700 Å (Table 2).

Table 2 summarizes the characteristics of ITO/PVK–PBD-phosphor/Mg–Ag/Ag devices prepared with **2** and **3** phosphors. Dopant concentrations in the range of 0.6–3.5% were examined for these devices with polymer layer thicknesses of 1300 Å. The ITO/PVK–PBD-phosphor/Mg–Ag/Ag mdpLEDs exhibit electroluminescence with peaks corresponding to the dopant emission maxima at 510 for **3** and 650 nm for **2** (Fig. 4). No contribution from PVK emission is observed in the EL spectra indicating efficient exciton trapping on the dye centers. A peak quantum efficiency of 0.62% was achieved at ≈2% doping of **2**. mdpLEDs with **3** gave external quantum efficiencies of 1.8% at doping levels of 3–3.5%. This efficiency is higher than the efficiencies achieved in fluorescent dye doped polymer LEDs and comparable to devices prepared with a Irppy doped PVK hole transporting layer and an Alq_3 electron transporting/injecting layer [13]. We attribute the high efficiency to the favorable combination of three factors: (1) the triplet character of emission, (2) a high quantum yield of phosphorescence and (3) a relatively short emission lifetime. Decay of electrophosphorescent devices efficiency as a function of current density appears to be independent of the dopant concentration in PVK–PBD-phosphor devices. As an example, external quantum efficiencies of FIrppy devices as a function of current density are shown in Fig. 5(a). 0.7%, 1.4%, 2.2% and 3.5%-doped PVK–PBD–FIrppy LEDs show similar rates of decay in efficiency as the current density is increased (after reaching a maximum efficiency between 20 and 50 mA cm^{-2}). A similar trend is observed for $Pt(thpy)_2$ and PtOX-based devices.

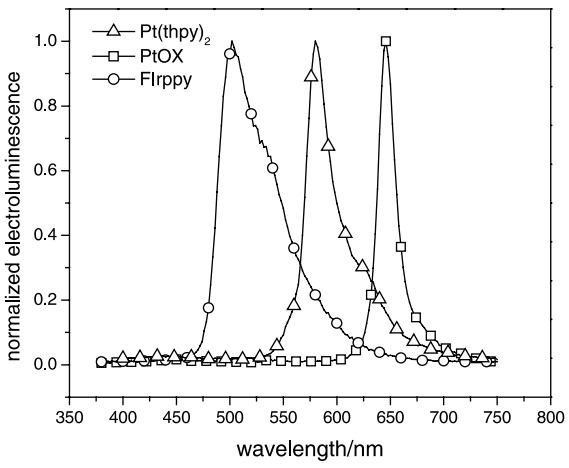

Fig. 4. Electroluminescence spectra of single layer ITO/PVK–PBD–dye/Mg–Ag/Ag devices with $Pt(thpy)_2$ (**1**), PtOX (**2**) and FIrppy (**3**) as dyes. All spectra were taken at applied voltage in the range of 15–18 V.

3.3. Molecularly doped polymer/organic heterostructure LEDs

Some mdpLED systems have been shown to exhibit injection limited electroluminescence [35]. In order to determine if the cathode is suffering from poor electron injection, we have prepared devices with a well known injecting layer, i.e. Alq_3 (**6**, Fig. 1). mdpLEDs of the general formula ITO/PVK–PBD–dye/Alq_3/Mg–Ag/Ag have been prepared with $Pt(thpy)_2$ (**1**), PtOX (**2**) and FIrppy (**3**). Dye concentrations were chosen close to optimal ones as determined from single-layer device studies: 3.3, 2.1 and 3.5 wt.% for **1**, **2** and **3**, respectively. Under chosen deposition conditions, doped polymer and Alq_3 formed films with thicknesses of 1300 and 250 Å, respectively.

Fig. 5(b) shows quantum efficiency and luminance characteristics for all three heterostructures. Alq_3-capped mdpLEDs exhibit turn on voltages in the range of 7.5–12 V, similar to the corresponding single layer devices (Table 3). Increased peak efficiency of the mdp/organic heterostructures compared to their single layer analogues suggests there is better charge balance in the heterostructures. Considering that hole mobility of PVK is not likely to limit mdpLED performance [35], either poor hole injection from ITO anode to PVK or low electron mobility in PBD may be responsible for high turn on voltages and operation voltages of these devices. At voltages of 12–20 V PVK–PBD–dye/Alq_3 LEDs show peak quantum efficiency of 2.2% (6.0 Cd/A), 1.8% (1.02 Cd/A) and 2.8% (8.5 Cd/A) for **1**–**3**-doped structures, respectively (Fig. 5(b), Table 3).

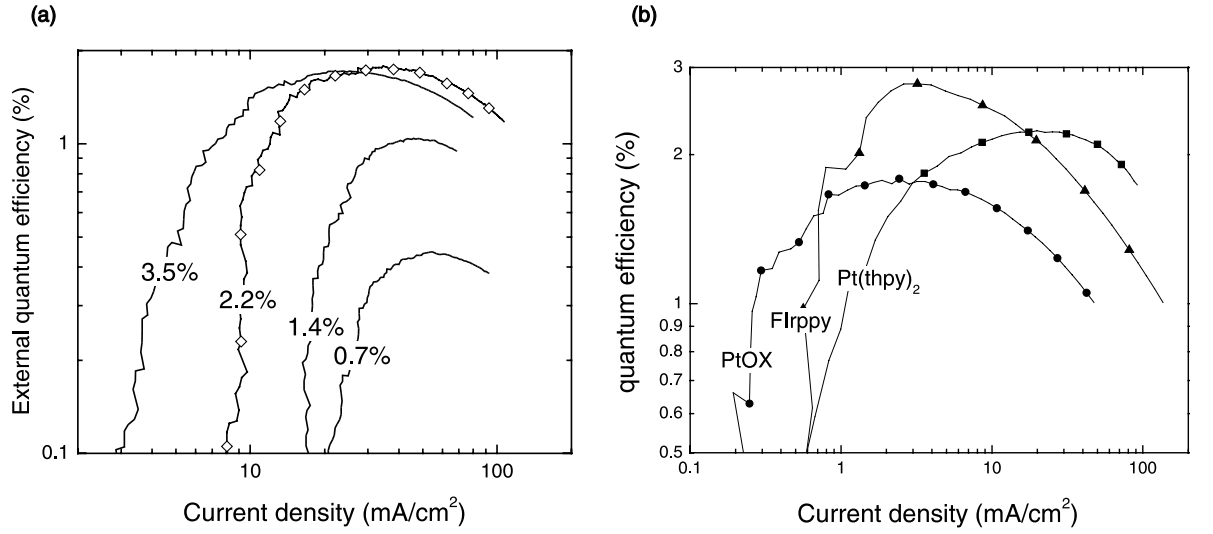

Fig. 5. External quantum efficiency of (a) single layer ITO/PVK–PBD–FIrppy/Mg–Ag/Ag mdpLEDs at different concentrations of FIrppy (indicated in the graph for each trace) and of (b) the heterostructure mdpLEDs ITO/PVK–PBD–dye/Alq_3/Mg–Ag/Ag with $Pt(thpy)_2$ (**1**), PtOX (**2**) and FIrppy (**3**) at their optimal doping concentrations, 3.3%, 2.1% and 3.5%, respectively.

Table 3
Characteristics of ITO/PVK–PBD–dye (**1**, **2** or **3**) (1300 Å)/Alq_3/Mg:Ag/Ag mdpLEDs. All efficiencies listed are external efficiencies

Compound	Turn on voltage, V	Quantum efficiency, %	Luminance efficiency, Cd/A
1	10	2.2	6.0
2	12	1.8	1.02
3	7.5	2.8	8.5

After reaching its maximum, the quantum efficiency drops with increasing current density, as observed for other phosphorescent OLEDs. Surprisingly, the rate of decrease is similar for mdpLEDs with **1** and **3,** showing relatively short-lived phosphorescence (1.5–2.0 μs, Table 1), and for those with **2** that exhibits a much longer emission lifetime (76 μs, Table 1). The independence of the efficiency decay rate on either dopant concentration or lifetime cannot be rationalized by increased triplet–triplet annihilation *between the dopant molecules* as the current is increased, as is normally proposed [34]. The triplet energies for PVK and dopants **2** and **3** are very similar (*vide supra*) [32], so back energy transfer from the dopant to PVK, followed by triplet–triplet annihilation in the PVK matrix could be occurring and would account for the observed independence of the efficiency decay on lifetime and dopant concentration [36,37]. Even under such circumstances no emission from PVK in the devices is expected, due to the low efficiency of its room temperature phosphorescence [32]. An alternate process could also be responsible for the efficiency decrease, which may not show lifetime or concentration dependence. The dopant bound excitons could be quenched by interaction with a trapped charge (hole or electron on an adjacent molecule). Exciton/trapped charge quenching has been observed in organic materials in general [38] and for PtOEP in particular [39]. This quenching process would be expected to show a strong current density dependence, being most severe at high currents, where the concentration of trapped charges in the thin film is the highest.

Interestingly, for all dopants electroluminescence spectra of the devices do not show any significant contribution from either Alq_3 or from polymer host material, and match those of single layer devices (Fig. 4). This demonstrates that hole leakage into Alq_3 layer is minimal and does not lead to any measurable exciton recombination on aluminum quinolate molecules. The lack of Alq_3 emission is indicative of efficient hole trapping on

the phosphorescent dye dispersed in PVK and efficient electron injection from Alq_3 into the doped polymer layer, as discussed below.

3.4. Electrochemistry: mechanisms of exciton formation in phosphorescent mdpLEDs

Both single- and double-layer mdpLEDs prepared with **1** exhibit yellow–orange electroluminescence centered at 580 nm (Fig. 4). The EL spectrum is independent of applied voltage (14–22 V) for all of the doping levels examined here (2–4%). Unlike the photoluminescence from PVK-**1** thin film (Fig. 2), the device EL spectra exhibit a negligible blue contribution at 410–425 nm, attributed to the host emission. Moreover, the dye concentration corresponding to the peak electroluminescence efficiency (≈3.3% by weight, Table 2) is noticeably lower than the concentration of **1** in PVK-**1** thin films that gives the most efficient energy transfer to the dye (6%, Fig. 2). These two differences in the EL and PL behavior of the films suggest that exciton formation on the dopant centers in the devices does not result only from simple singlet–singlet and triplet–triplet energy transfer from the host, but also results from charge trapping processes at the dopant.

In order to probe if charge trapping (hole and/or electron trapping) by **1**, **2** or **3** in a PVK matrix is likely, we examined electrochemistry of the dyes. The electrochemical behavior of **1** has been reported and consists of an irreversible oxidation wave with $E_{1/2} = +0.74$ V versus SCE and two reversible reduction waves with $E_{1/2} = -1.75$ V and -2.07 V versus SCE [40]. [4] Cyclic voltametric analysis of **2** and **3** shows reversible oxidation waves at 1.0 and 0.94 V versus SCE, respectively. Reduction potentials are estimated to be greater than -2.0 V (no reduction wave was observed in benzonitrile solution). If the oxidation potential of the phosphor dopant is significantly less than that of PVK, holes will be efficiently transferred to the phosphor and potentially trapped there. The oxidation potential for PVK is 1.2 V versus SCE [16], suggesting that holes will be efficiently transferred to the phosphor for all three dopants. At the lower doping concentrations used here (1–4%) we expect the holes will be trapped at the dopant. The concentrations in this regime are low enough that carrier hopping between dopants will most likely not be facile. At higher concentrations inter-dopant hopping may be possible and may be an important hole conduction pathway in these doped PVK films. Considering that charges are likely to be trapped at the phosphorescent dopants, carrier recombination at the dopant may be a significant pathway to exciton formation at the dopant. In this recombination process a phosphor bound carrier (hole or electron) would recombine with an opposite carrier on an adjacent site (PVK segment or PBD) to give the phosphor bound exciton. Similar charge trapping behavior was proposed for some fluorescence-based PVK mdpLEDs [41]. Exciton formation at the phosphor dopants in the phosphorescence-based mdpLEDs can proceed via either (a) energy transfer from the host matrix to the dye or (b) hole and electron trapping by the dopant, followed by dopant/matrix carrier recombination. The absence of any PVK emission in the EL spectra of films that have strong contributions from PVK in their PL spectra, suggests that the latter process is a significant contributor to the overall EL emission.

[4] Refer to Table 1, footnote a.

4. Conclusion

The high electroluminescence efficiency obtained from phosphorescent dye doped polymer LEDs demonstrates that the use of phosphorescent dopant can significantly increase polymer LED efficiencies, just as these dopants increase efficiencies of small molecule based OLEDs. We have achieved ≈0.6% external quantum efficiency in $Pt(thpy)_2$ and PtOX based devices and ≈1.8% efficiency in FIrppy single-layer devices due to a combination of higher phosphorescence yield and lower emission lifetime of the phosphorescent dopant. Introduction of a better electron injecting contact Alq_3/Mg:Ag leads to a substantial increase in efficiency of the devices. Heterostructure LEDs exhibit 1.8–2.8% quantum efficiency for all studied dopants at very low currents. Persisting high

voltages of turn on and operation may be consequences of low electron mobility in PBD or/and poor carrier injection. The second order quenching process present in these OLEDs, which is prevalent at high current densities, is most likely not due to T–T annihilation of excitons trapped at dopant sites in these OLEDs. T–T annihilation in the PVK matrix or trapped charge-triplet annihilation are more likely explanations for the decrease. Although energy transfer from the host material (PVK) to the dyes is evidently a mechanism of exciton formation on the phosphor centers, our results suggest that charge trapping by the dopant molecules is also very important.

Acknowledgements

This work was supported by Universal Display Corporation, Defense Advanced Research Projects Agency, the Airforce Office of Scientific Research through Multidisciplinary University Research Institution (MURI) program, and National Science Foundation.

References

[1] D. Kalinowski, J. Phys. D: Appl. Phys. 32 (1999) R179.
[2] M.E. Thompson, P.E. Burrows, S.R. Forrest, Current Top. Solid State Mater. Sci. 4 (1999) 369.
[3] M.A. Baldo, D.F. O'Brien, Y. You, A. Shoustikov, S. Sibley, M.E. Thompson, S.R. Forrest, Nature 395 (1998) 151.
[4] C. Adachi, M. Baldo, S.R. Forrest, M.E. Thompson, Appl. Phys. Lett. 77 (2000) 904.
[5] M.A. Baldo, S. Lamansky, P.E. Burrows, M.E. Thompson, S.R. Forrest, Appl. Phys. Lett. 75 (1999) 4.
[6] M.A. Baldo, D.F. O'Brien, M.E. Thompson, S.R. Forrest, Phys. Rev. B 60 (1999) 14422.
[7] Y. Cao, I.D. Parker, G. Yu, C. Zhang, A.J. Heeger, Nature 397 (1999) 414.
[8] V. Cleave, G. Yahioglu, P. Le Barny, R.H. Friend, N. Tessler, Adv. Mater. 11 (1999) 285.
[9] G. Gu, D.Z. Garbuzov, P.E. Burrows, S. Venkatesh, S.R. Forrest, M.E. Thompson, Opt. Lett. 22 (1997) 396.
[10] J.H. Burroughes, D.D.C. Bradley, A.R. Brown, R.N. Marks, K. Mackay, R.H. Friend, P.L. Burns, A.B. Holmes, Nature 347 (1990) 539.
[11] M. Berggren, O. Inganäs, G. Gustafsson, J. Rasmusson, M.R. Andersson, T. Hjertberg, O. Wennerstrom, Nature 372 (1994) 444.
[12] A. Wu, D. Yoo, J.K. Lee, M.F. Rubner, J. Am. Chem. Soc. 121 (1999) 4883.
[13] M.J. Yang, T. Tsutsui, Jpn. J. Appl. Phys. 39 (2000) L828.
[14] J. Kido, M. Kohda, K. Okuyama, K. Nagai, Appl. Phys. Lett. 61 (1992) 17.
[15] W.D. Gill, J. Appl. Phys. 43 (1972) 5033.
[16] C. Wu, J.C. Sturn, R.A. Register, J. Tian, E.P. Dana, M.E. Thompson, IEEE Trans. Electron. Dev. 44 (1997) 1269.
[17] R. Zhang, H. Zheng, J. Shen, Synth. Met. 105 (1999) 49.
[18] J.S. Huang, H.F. Zhang, W.J. Tian, J.Y. Hou, Y.G. Ma, J.C. Shen, S.Y. Liu, Synth. Met. 87 (1997) 105.
[19] C. Liang, W. Li, Z. Hong, X. Liu, J. Peng, L. Liu, Z. Lu, M. Xie, Z. Liu, J. Yu, D. Zhao, Synth. Met. 91 (1997) 151.
[20] Y. Ma, H. Zhang, J. Shen, C. Che, Synth. Met. 94 (1998) 245.
[21] J. Kido, W. Ikeda, M. Kimura, K. Nagai, Jpn. J. Appl. Phys. Part 2 – Lett. 35 (1996) L394.
[22] Y. Ma, C. Che, H. Chao, X. Zhou, W. Chan, J. Shen, Adv. Mater. 11 (1999) 852.
[23] R.C. Kwong, S. Sibley, T. Dubovoy, M. Baldo, S.R. Forrest, M.E. Thompson, Chem. Mater. 11 (1999) 3709.
[24] M.G. Colombo, A. Hauser, H.U. Gûdel, Top. Curr. Chem. 171 (1994) 143.
[25] L. Chassot, A. von Zelewsky, Inorg. Chem. 26 (1987) 2814.
[26] E.-I. Negishi, F.-T. Luo, R. Frisbee, H. Matsushita, Heterocycles 18 (1982) 117.
[27] K. Dedeian, P.I. Djurovich, F.O. Garces, G. Carlson, R.J. Watts, Inorg. Chem. 30 (1991) 1685.
[28] K.A. King, P.J. Spellane, R.J. Watts, J. Am. Chem. Soc. 107 (1985) 1431.
[29] T.-F. Guo, S.-C. Chen, Y. Yang, R.C. Kwong, M.E. Thompson, Organic Electronics 1 (2000) 15.
[30] H. Tokuhisha, M. Era, T. Tsutsui, S. Saito, Appl. Phys. Lett. 66 (1995) 3433.
[31] G. Rippen, G. Kaufmann, W. Klöpffer, Chem. Phys. 52 (1980) 165.
[32] R.D. Burkhart, Macromolecules 16 (1983) 820.
[33] A.A. Shoustikov, Y.J. You, M.E. Thompson, IEEE J. Sel. Top. Quant. 4 (1998) 3.
[34] R.C. Kwong, S.A. Lamansky, M.E. Thompson, Adv. Mater. 12 (2000) 1134.
[35] G.E. Johnson, K.M. McGrane, M. Stolka, Pure Appl. Chem. 67 (1995) 175.
[36] C. Adachi, M.A. Baldo, S.R. Forrest, J. Appl. Phys. 87 (2000) 8049.
[37] M.A. Baldo, S.R. Forrest, Phys. Rev. B 62 (2000) 10958.
[38] M. Pope, C.E. Swenberg, Electronic Processes in Organic Crystals, Oxford University Press, Oxford, 1982, p. 515.
[39] M.A. Baldo, C. Adachi, S.R. Forrest, Phys. Rev. B 92 (2000) 10967.
[40] S. Bonafede, M. Ciano, F. Bolletta, V. Balzani, L. Chassot, A. von Zelewsky, J. Phys. Chem. 90 (1986) 3836.
[41] M. Uchida, C. Adachi, T. Koyama, Y. Taniguchi, J. Appl. Phys. 86 (1999) 1680.